

# Exploration of the Intriguing Photovoltaic Behavior for Fused Indacenodithiophene-Based A–D–A Conjugated Systems: A DFT Model Study

Muhammad Nadeem Arshad, Iqra Shafiq, Muhammad Khalid,\* and Abdullah M. Asiri



Cite This: *ACS Omega* 2022, 7, 11606–11617



Read Online

ACCESS |



Metrics & More

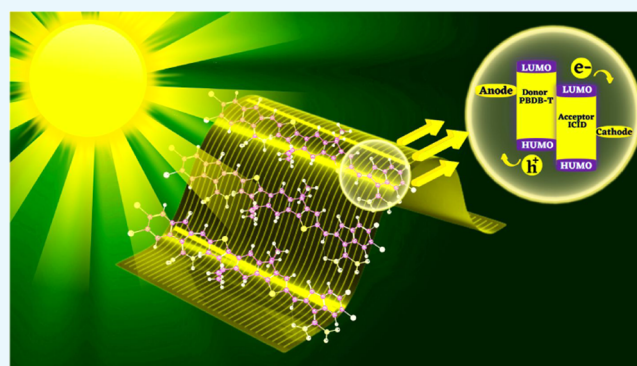


Article Recommendations



Supporting Information

**ABSTRACT:** Many researchers are engaged nowadays in developing efficient photovoltaic materials to accomplish the demand of modern technology. Nonfullerene small molecular acceptors (NF-SMAs) show potential photovoltaic performance, accelerating the development of organic solar cells (OSCs). Herein, the first theoretical designing of a series of indacenodithiophene-based (IDIC1–IDIC6) acceptor chromophores was done by structural tailoring with various well-known acceptors from the recently synthesized IDICR molecule. For the selection of the best level of density functional theory (DFT), various functionals such as B3LYP, M06-2X, CAM-B3LYP, and  $\omega$ B97XD with the 6-311G(d,p) basis set were used for the UV–visible analysis of IDICR. Consequently, UV–visible results revealed that an interesting agreement was found between experimental and DFT-based values at the B3LYP level. Therefore, quantum chemical investigations were executed at the B3LYP/6-311G(d,p) level to evaluate the photovoltaic and optoelectronic properties. Structural tailoring with various acceptors resulted in a narrowing of the energy gap (2.245–2.070 eV) with broader absorption spectra (750.919–660.544 nm). An effective transfer of charge toward lowest unoccupied molecular orbitals (LUMOs) from highest occupied molecular orbitals (HOMOs) was studied, which played a crucial role in conducting materials. Further, open circuit voltage ( $V_{oc}$ ) analysis was performed with respect to  $HOMO_{PBD-T} - LUMO_{ACCEPTOR}$ , and all of the derivatives exhibited a comparable value of voltage with that of the parent chromophore. Lower reorganization energies in titled chromophores for holes and electrons were examined, which indicated the higher rate of mobility of charges. Interestingly, all of the designed chromophores exhibited a preferable optoelectronic response compared to the reference molecule. Therefore, this computed framework demonstrates that conceptualized chromophores are preferable and might be used to build high-performance organic solar cells in the future.



## INTRODUCTION

In the current era, one of the world's major issues is energy crisis. This has emerged due to large dependence on nonrenewable energy sources, which will be exhausted sooner or later and which causes environmental problems due to combustion.<sup>1</sup> Many alternatives such as hydropower, biomass, wind power, and solar cells have been discovered to tackle this problem. Of all of these resources, solar cells have proved to be the best choice due to the vast amount of sunlight available. Silicon with high thermal stability, low toxicity, and high efficiency of about 46% has been utilized as a semiconductor material in SCs for decades.<sup>2,3</sup> However, there are certain drawbacks associated with silicon-based solar cells including nontunable energy levels, hardness, and high cost with manufacturing difficulty.

Since then, scientists have found OSCs to be an alternative to silicon-based solar cells. Organic solar cells have been given preference over silicon-based SCs due to their low manufacturing cost, light weight, high flexibility, tunable energy levels, and

high power conversion efficiency.<sup>4</sup> Moreover, OSCs have been developed rapidly in the last couple of years owing to their environment-friendly nature. Therefore, OSCs have attracted extensive attention and maximized use, especially in sunny areas, due to the large and uninterrupted availability of light. The mechanism and working of solar cells are based on the photoelectric effect that converts sunlight directly into electricity. Generally, OSCs are made up of electrodes and an active layer of organic solar cells (OSCs), composed largely of electron-donor and electron-acceptor counterparts.<sup>5</sup> Upon interaction of electromagnetic radiations with the active layer, electrons travel from HOMO to LUMO.<sup>6</sup> Organic solar cells

Received: November 5, 2021

Accepted: March 15, 2022

Published: March 29, 2022



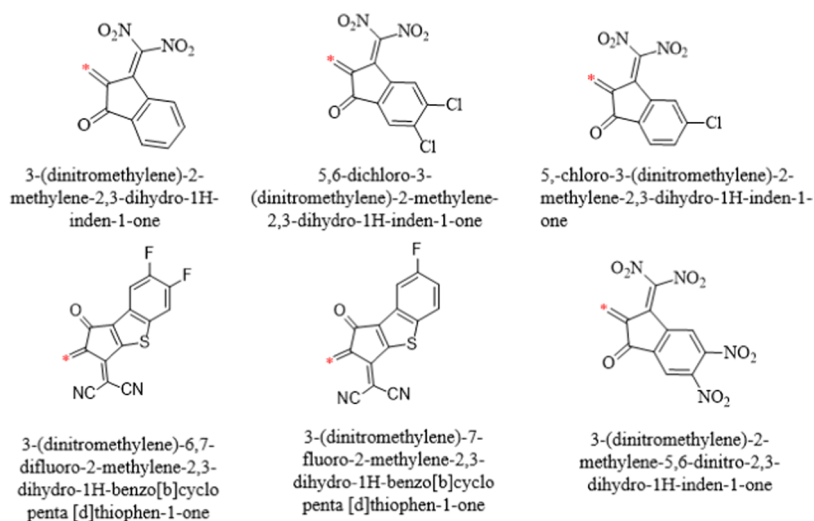


Figure 1. IUPAC names and structural representation of acceptors.

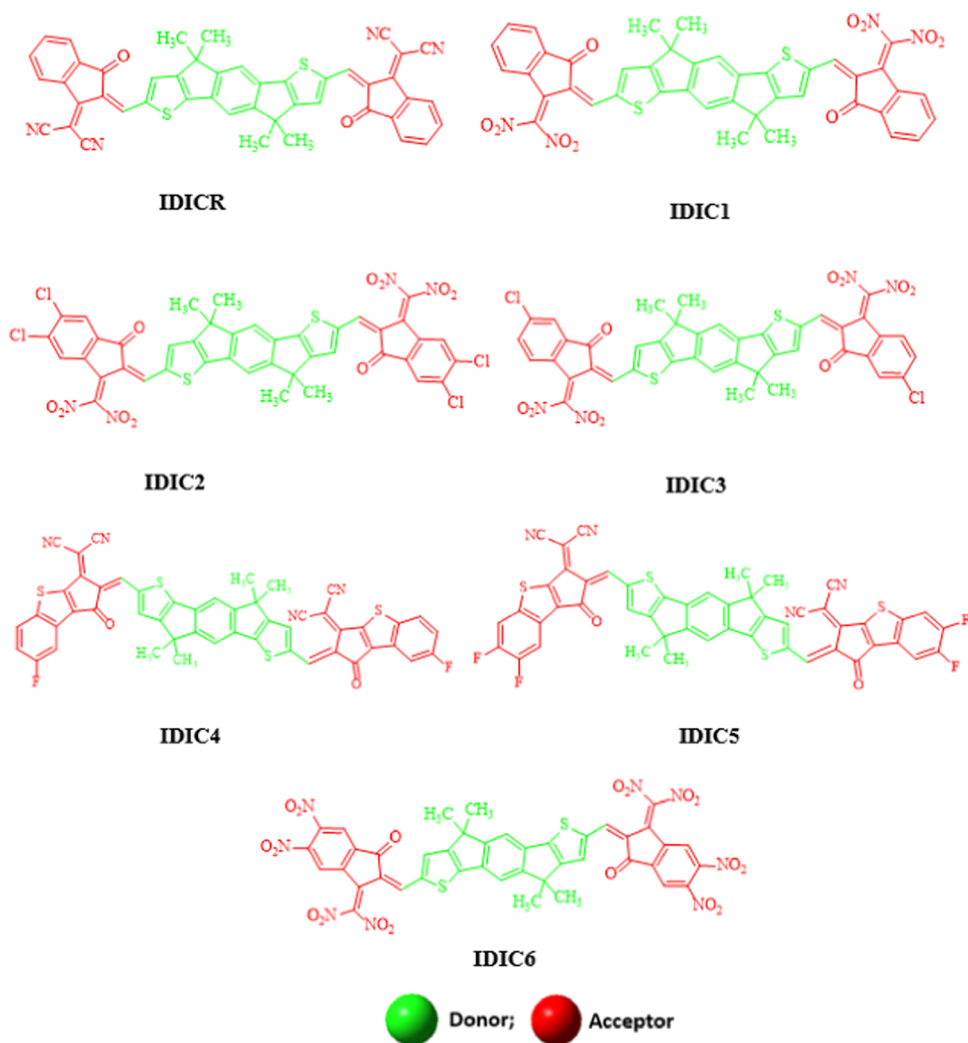


Figure 2. 2D structural view of the reference and designed chromophores.

blended with fullerene acceptors (FAs) exhibit a power conversion efficacy of 11–12% in the bulk heterojunction (BHJ).<sup>7,8</sup> Fullerene derivatives (PC<sub>61</sub>BM and PC<sub>71</sub>BM) blended with organic solar cells show tremendous properties such as low reorganization energies, high electron mobility,

and isotropic charge transfer.<sup>5,9</sup> On large-scale use, fullerene-based OSCs have certain limitations such as low absorption in the visible region, low  $V_{oc}$ , high band gap, high cost, and a limited number of energy levels.<sup>10,11</sup> To address these limitations and to make solar cells more effective, scientists

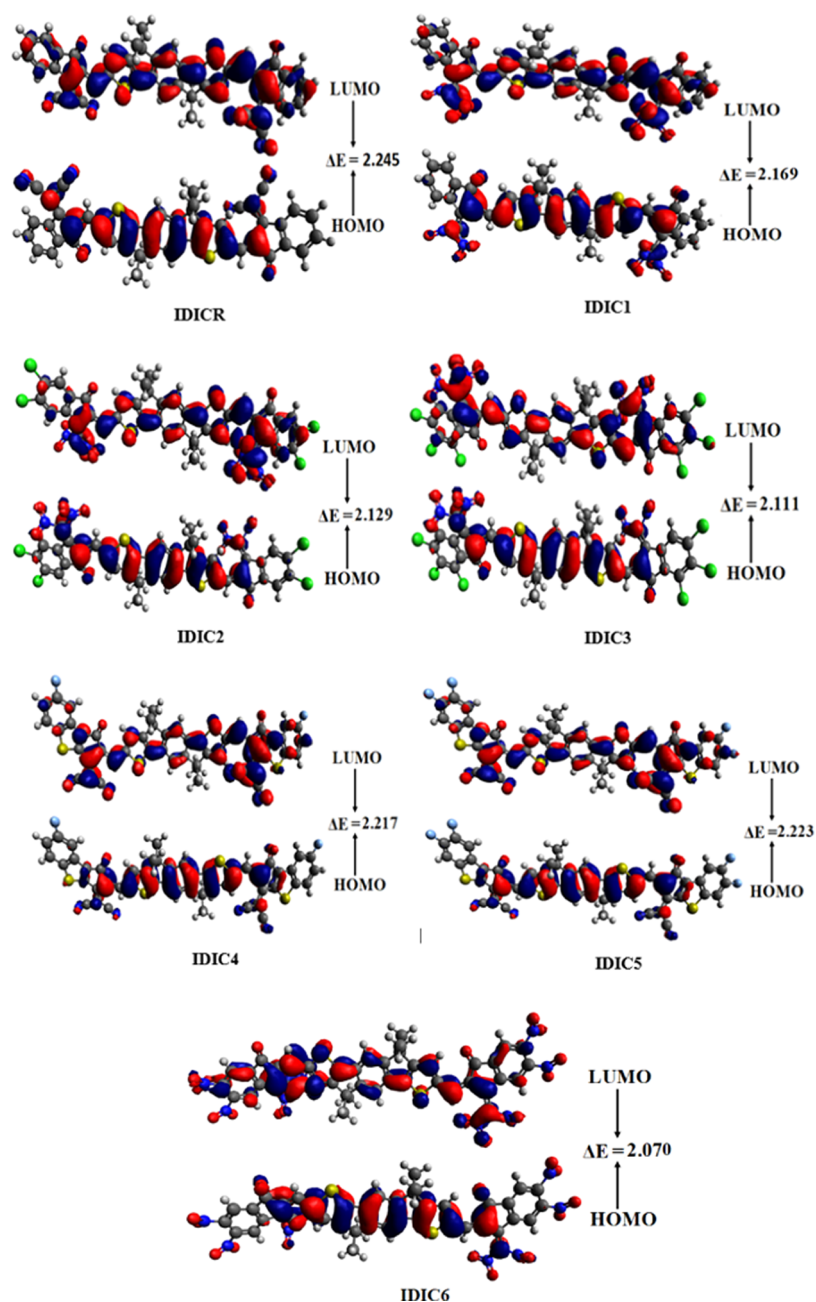


Figure 3. HOMOs and LUMOs of titled chromophores.

have been working to design and synthesize non-fullerene-based organic solar cells.<sup>12–14</sup> Recently, fullerene-free organic solar cells have been classified into two categories: small molecular acceptor (SMA) solar cells and polymer solar cells. Small molecular acceptor solar cells have better optoelectronic properties than polymer solar cells.<sup>15–17</sup> A wide variety of constructional design foundations is offered by NFA molecules; however, the A–D–A-fashioned molecules are largely employed by implementing special core pieces (acting as donors), linkers, and terminal groups (acting as acceptors).<sup>18–22</sup> Literature surveys show many studies that yield SCs based on small molecules, such as X-shaped donor molecules,<sup>23</sup> star-shaped molecules,<sup>24</sup> and linear geometric molecules.<sup>25</sup> Moreover, the extended  $\pi$ -conjugation with fullerene-free compounds with intense absorption parameters has been improved via attachment with fluoro,<sup>26</sup> cyano, and

chloro units over the NFA skeleton.<sup>27</sup> In this article, we have designed seven new A–D–A-type chromophores, namely, IDIC1–IDIC6, from a reference compound IDIC-C8<sup>28</sup> represented as IDICR. All of the new compounds have been designed by changing the terminal acceptor unit of reference chromophores containing two 2-(2,3-dihydro-3-oxo-1*H*-inden-1-ylidene) propanedinitrile (IC) units attached at the terminal with an electron-donating core, indacenodithiophene (IDT). We studied the impact of various terminal acceptor units on the electronic, optical, and charge transfer behavior of the newly designed acceptor chromophores to evaluate them as efficient OSC-based compounds for future fabrication of high-performance electronic devices.

## RESULTS AND DISCUSSION

In the present study, IDICR is utilized as a parent chromophore consisting of an indacenodithiophene (IDT) core that acts as a D moiety, flanked by an acceptor (A), 2-(2,3-dihydro-3-oxo-1*H*-inden-1-ylidene) propanedinitrile. We substituted the end-capped acceptor of IDICR with different reported acceptors (Figure 1) to design IDIC1–IDIC6 chromophores (Figure 1) for exploration of the effect of various acceptors on the photophysical and optoelectronic properties. Moreover, we calculated the Gibbs free energy for the derivatives to determine their synthesis and storage. Negative values of Gibbs free energy have been calculated (see Table S15) for each reaction, which indicates that these new systems could be synthesized and stored in the laboratory (Figure 2).

**Frontier Molecular Orbital (FMO) Analysis.** The distribution pattern of FMOs provides helpful visuals and numbers for the characterization of photovoltaic and optoelectronic behavior of chromophores in OSCs.<sup>29</sup> Intermolecular charge transfer (ICT), chemical stability, reactivity, and molecular interactions also come under the scope of FMOs<sup>30</sup> and can be well explained through this tool.<sup>31</sup> Pictorial representation of the molecular orbitals of all studied chromophores at the B3LYP/6-311G(d,p) level of theory is exhibited in Figure 3, and computed results are tabulated in Table 1. The highest occupied molecular orbitals (HOMOs)

**Table 1.**  $E_{\text{HOMO}}$ ,  $E_{\text{LUMO}}$ , and Energy Gap of Studied Molecules<sup>a</sup>

compounds	HOMO ( $E_{\text{HOMO}}$ )	LUMO ( $E_{\text{LUMO}}$ )	$E_{\text{gap}}$
IDICR	−5.948	−3.703	2.245
IDIC1	−6.018	−3.849	2.169
IDIC2	−6.233	−4.104	2.129
IDIC3	−6.265	−4.154	2.111
IDIC4	−5.944	−3.727	2.217
IDIC5	−6.008	−3.785	2.223
IDIC6	−6.628	−4.558	2.07

<sup>a</sup>Units are in eV.

and lowest unoccupied molecular orbitals (LUMOs), termed as quantum orbitals, have the ability to donate and accept electrons, respectively.<sup>32</sup> Band theory showed that the HOMO and LUMO of chromophores are also characterized as the valance and conduction bands, respectively.<sup>30,33–36</sup> The difference of energy between the occupied and unoccupied orbitals is recognized as the band-gap energy gap ( $E_{\text{gap}}$ ), which provides valuable information regarding the performance of OSCs.<sup>37,38</sup> Open circuit voltage and power conversion efficiency can be well estimated on the basis of energy gap. The smaller the  $E_{\text{gap}}$ , the greater the effectiveness and vice versa.

As illustrated in Table 1, the calculated HOMO and LUMO energies of IDICR are −5.948 and −3.703 eV, comprising a band gap of 2.245 eV, comparable with the experimental value (1.77 eV).<sup>28</sup> This good agreement points out that the implemented DFT computation, i.e., B3LYP functional, is suitable for use to investigate IDIC1–IDIC6. The HOMO energy values of IDIC1, IDIC2, IDIC3, IDIC4, IDIC5, and IDIC6 are calculated to be −6.018, −6.233, −6.265, −5.944, −6.008, and −6.628 eV, respectively. Consequently, the computed  $E_{\text{LUMO}}$  values for the designed molecules (IDIC1–IDIC6) are found to be −3.849, −4.104, −4.154, −3.727,

−3.785, and −4.558 eV, respectively. The computed HOMO–LUMO band-gap values of IDIC1–IDIC6 are 2.169, 2.129, 2.111, 2.217, 2.223, and 2.070 eV, respectively. Relatively, a decrease in band gap is noticed in the designed compounds as compared to IDICR. The  $E_{\text{gap}}$  between HOMO and LUMO becomes narrow in IDIC5 and IDIC4 (2.223 and 2.217 eV, respectively) when electron-withdrawing fluoro groups are introduced in terminal A units. Similarly, among IDIC1 and IDICR, a reduction in the band gap is observed when replacing the cyano (−CN) group with a nitro group. This might be due to an increase in resonance and the strongly deactivating nature of the nitro group.<sup>39</sup> The band gap further decreased from 2.169 to 2.129 eV in IDIC2 when halo groups (−Cl) were incorporated in end-capped acceptor units. Consequently, the electronic cloud migrated toward A moiety in these chromophores due to the strong electron-accepting nature of nitro and chloro groups, which might be a reason for a further decrease in their energy gap. On increasing the number of chloro units on acceptor moieties, the band gap further decreased (2.111 eV) in IDIC3. In IDIC6 chromophore, the lowest band gap is observed among all of the derivatives as halo groups are replaced with a strong electron-withdrawing nitro group (−NO<sub>2</sub>). The strong electron-withdrawing effect along with enhancement in resonance causes the reduction in the band gap of IDIC6 molecules. The descending order of energy gap is found to be IDICR > IDIC5 > IDIC4 > IDIC1 > IDIC2 > IDIC3 > IDIC6. The lower value of LUMO generates a lower band gap in all designed molecules, leading to easy charge transfer and thus enhancing the photovoltaic properties of OSCs. For charge transfer analysis, energy gap is a significant factor. The HOMO–LUMO energy difference influences the charge transfer (CT) rate; the smaller the band gap, the larger the charge transfer ability and vice versa.<sup>40,41</sup> Moreover, the electron density distribution patterns on the surfaces (LUMO/HOMO) of IDICR and its designed chromophores are shown in Figure 3. The electronic cloud for HOMO in IDICR and IDIC1–IDIC6 is significantly located over the central donor indacenodithiophene (IDT) and slightly on the acceptor, except for terminal benzene rings, while the LUMO electron density is concentrated dominantly all over the chromophore. In a nutshell, the above discussion explicates that the modification of acceptor groups with strong electron-withdrawing units created a relatively smaller band gap between orbitals and efficient CT toward A from D, which shows them to be efficient materials for OSCs.

**Density of State (DOS).** DOS helps to support the outcomes elaborated in FMO diagrams (Figure 3). DOS spectra of the studied compounds are displayed in Figure 4, which clearly show that the powerful electron-withdrawing nature of the A moieties alters the distribution arrangement around the HOMO and LUMO. To explicate the DOS study, we divided our chromophores into two parts, i.e., donor (the core unit) and acceptor (the end-capped group), which are displayed by red and green lines, respectively. Along the *x*-axis, the negative values in DOS graphs indicate the valence band (HOMO), while positive values indicate the conduction band (LUMO), and the distance between HOMO and LUMO denotes the energy gap.<sup>42</sup> For IDICR the acceptor contributes 34.3% to HOMO and 63.3% to LUMO, while the donor contributes 65.7% to HOMO and 36.7% to LUMO. Similarly, the acceptor contributes 33.9, 34.5, 34.9, 31.9, 31.8, and 35.5% to HOMO and 69.8, 70.3, 70.7, 75.6, 75.6, and 72.7% to

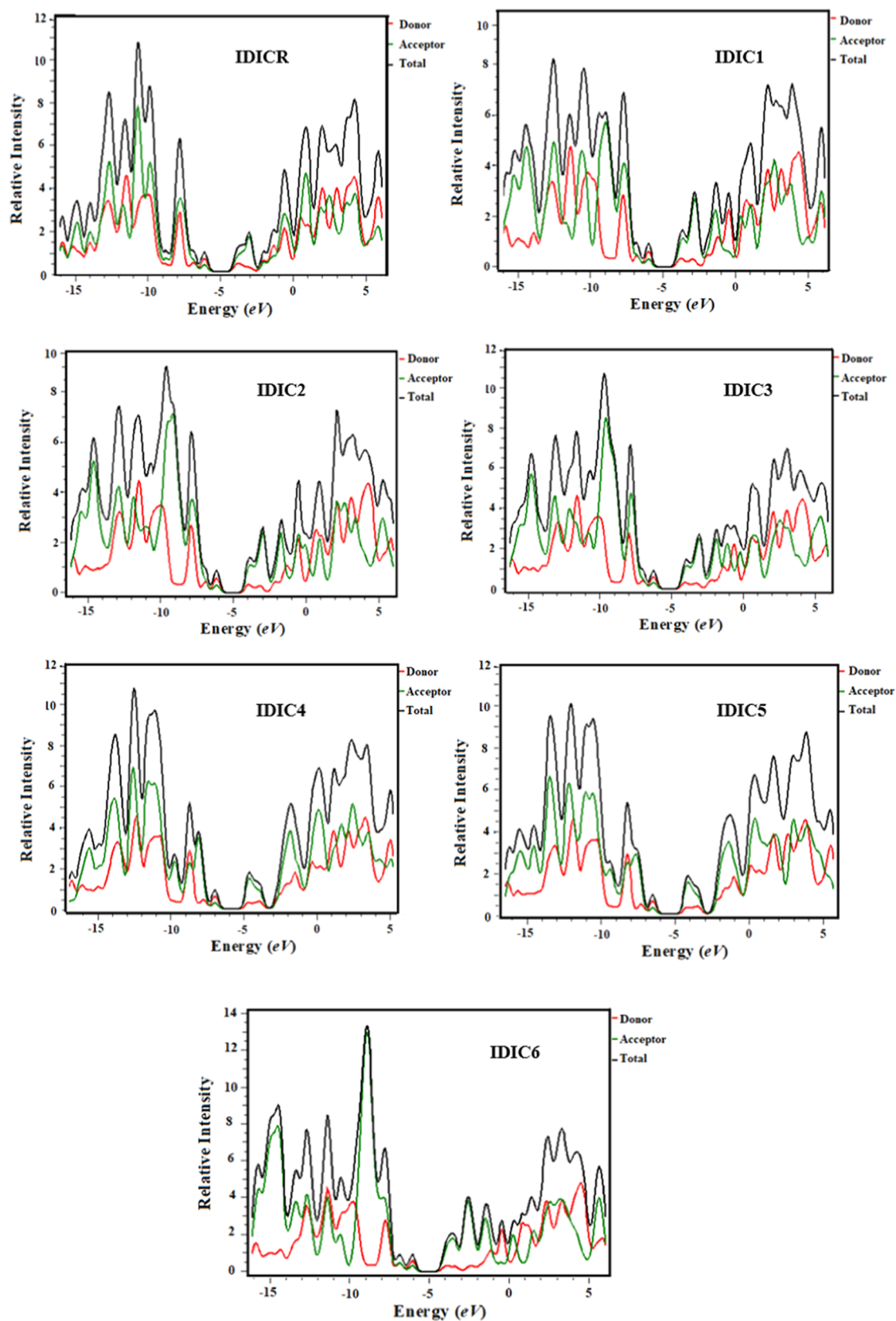


Figure 4. Graphical representation of DOS of titled chromophores.

LUMO in IDIC1–IDIC6, respectively. In the same way, the donor contributes 66.1, 65.5, 65.1, 68.1, 68.2, and 64.5% to HOMO and 30.2, 29.7, 29.3, 24.4, 24.4, and 27.3% to LUMO for IDIC1–IDIC6, respectively. From the complete discussion,

it was observed that the HOMOs of the aforesaid chromophores are largely concentrated on the D moiety while the LUMOs are significantly present on A units. Hence, DOS graphs considerably support the FMO diagrams (see

Figures 2 and 3). The DOS investigation showed that there was substantial delocalization of the electronic cloud and an enormous amount of charge was transferred from donor to acceptor groups.

**Optical Properties.** To demonstrate the working capability of OSCs, their photophysical responses were evaluated employing TD-DFT computations. To obtain insights into the optoelectronic properties, UV–visible spectra of the derivatives (IDIC1–IDIC6) were obtained in chloroform and gaseous phase at the B3LYP/6-311G(d,p) level of theory. Findings in the form of maximum absorbed wavelength  $\lambda_{\max}$ , excitation energy, assignments, and oscillator strength ( $f$ ) in solvent and gaseous phase are illustrated in Tables 2 and 3,

**Table 2. Computed Energy, Wavelength ( $\lambda_{\max}$ ), and Oscillator Strength of titled Chromophores in Chloroform<sup>a</sup>**

compounds	$\lambda_{\max}$ (nm)	$E$ (eV)	$f$	MO contributions
IDICR	660.544	1.877	2.323	H → L (98%)
IDIC1	706.261	1.756	1.831	H → L (98%)
IDIC2	723.024	1.715	1.943	H → L (98%)
IDIC3	727.820	1.704	1.939	H → L (98%)
IDIC4	695.798	1.782	1.547	H → L (96%)
IDIC5	694.979	1.784	1.536	H → L (96%)
IDIC6	750.919	1.651	1.641	H → L (98%)

<sup>a</sup>MO = molecular orbital, HOMO = H, LUMO = L, and  $f$  = oscillator strength.

**Table 3. Computed Excitation Energy, Wavelength ( $\lambda_{\max}$ ), and Oscillator Strength of IDICR and IDIC1–IDIC6 in Gaseous Phase<sup>a</sup>**

compounds	$\lambda_{\max}$ (nm)	$E$ (eV)	$f$	MO contributions
IDICR	613.449	2.021	2.058	H → L (98%)
IDIC1	642.672	1.929	1.670	H → L (98%)
IDIC2	656.766	1.888	1.810	H → L (98%)
IDIC3	661.567	1.874	1.807	H → L (98%)
IDIC4	648.249	1.913	1.295	H → L (94%)
IDIC5	647.877	1.914	1.278	H → L (94%)
IDIC6	674.487	1.838	1.582	H → L (97%)

<sup>a</sup>MO = molecular orbital, HOMO = H, LUMO = L, and  $f$  = oscillator strength.

respectively. It is commonly observed that electron-withdrawing groups cause an increase in the values of maximum absorbed wavelength  $\lambda_{\max}$ . Thus, the bathochromic shift in the absorption values is probably due to the addition of electron-withdrawing groups with extended conjugation.<sup>43</sup>

Maximum absorption values for derivatives lie in the range of 750.919–694.979 nm in chloroform, which are greater than that of IDICR (660.544 nm). There is good agreement between the absorption values of the simulated and experimental results (668 nm).<sup>28</sup> Among all designed molecules, the lower  $\lambda_{\max}$  has been observed in the case of IDIC1 when the –CN group of IDICR is replaced with a nitro group. This further enhancement in  $\lambda_{\max}$  is examined in IDIC1–IDIC5 when two halo groups are introduced on the terminal benzene ring of the acceptor. The combined electron-withdrawing nature of halo and –CN groups in IDIC1–IDIC5 reduced the  $E_g$  between orbitals and excitation energy with a wider absorption band. Interestingly, a higher red shift in absorption spectra has been observed when halo groups are replaced with cyano (–CN) groups. The strong electron-withdrawing –CN groups in IDIC6 have low excitation energy and low energy gap so that excitation from HOMO to LUMO is easy. The overall descending order of  $\lambda_{\max}$  of all studied compounds in solvent phase is IDIC6 > IDIC3 > IDIC2 > IDIC4 = IDIC5 > IDIC1 > IDICR.

The calculated  $\lambda_{\max}$  of all studied molecules in the gaseous phase is somewhat in the same order as that for the gaseous phase. However, a larger bathochromic shift is found in chloroform than in the gaseous phase, which might be due to the solvent effect. The absorption maximum of all investigated compounds in the gaseous phase is noted to be in the range of 642.672–674.487 nm. Findings involving the absorbed wavelength in the gaseous phase are listed in Table 3. From these investigations, it is found that all derivatives exhibited better optical properties compared to IDICR. Therefore, it has been proved that by the structural tailoring of the reference molecule with efficient acceptor moieties, chromophores with broader absorption spectra and reduced band gap could be obtained, which would be appealing OSC material (Figure 5).

**Reorganization Energy (RE).** Energy reorganization is considered to be one of the essential features, which is the reorganization of molecular structural correlations with com-

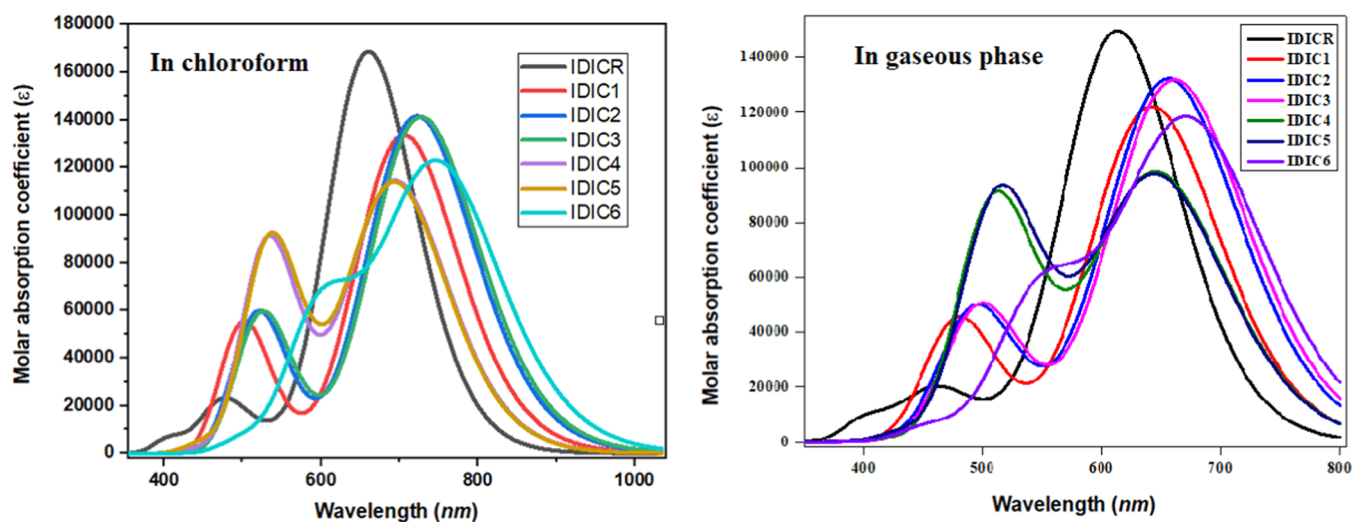


Figure 5. Stimulated absorption spectra of IDICR and IDIC1–IDIC6.

pounds' CT ability, to design the best possible applications for the solar cell industry. It aids in understanding the CT from D to A material. Chromophores with a low RE value exhibited larger photovoltaic effects, showing a higher magnitude of charge mobility. For solar cell materials, usually, two types of RE are noticed: external reorganization energy ( $\lambda_{\text{ext}}$ ) and internal reorganization energy ( $\lambda_{\text{int}}$ ). Herein, we neglected the  $\lambda_{\text{ext}}$  and the core focus was on  $\lambda_{\text{int}}$ . Thus, we have calculated the reorganization energies of IDICR and IDIC1–IDIC6

**Table 4. Computed Reorganization Energies of IDICR and IDIC1–IDIC6 Chromophores<sup>a</sup>**

compounds	$\lambda_e$	$\lambda_h$
IDICR	0.00047988	0.00019954
IDIC1	0.00022499	0.00037741
IDIC2	-0.00253835	0.00057392
IDIC3	-0.00200788	0.0005188
IDIC4	0.00052472	0.00019454
IDIC5	0.00056658	0.00022271
IDIC6	-0.00330809	0.00040764

<sup>a</sup> $\lambda_e$ : transfer rate of electrons and  $\lambda_h$ : transfer rate of holes.

molecules (Table 4) using eqs 1 and 2 for the assessment of the capacity of charge transfer.

$$\lambda_e = [E_0^- - E_-] + [E_0^0 - E_0] \quad (1)$$

$$\lambda_h = [E_0^+ - E_+] + [E_0^0 - E_0] \quad (2)$$

Herein,  $E_0^-$  and  $E_0^+$  are anionic and cationic energies, respectively, obtained from the optimized neutral configuration of a chromophore. Likewise,  $E_+^0$  and  $E_-^0$  are energies of a neutral chromophore calculated in the cationic and anionic states, respectively. Nevertheless,  $E_-$  and  $E_+$  represent the anionic and cationic optimized energies, respectively.  $E_0$  showed the ground-state single point energy.

The calculated RE values of the hole for IDICR is 0.00019954 eV while those for IDIC1–IDIC6 are 0.00037741, 0.00057392, 0.0005188, 0.00019454, 0.00022271, and 0.00040764 eV, respectively. The descending order of  $\lambda_h$  for the studied chromophores is IDIC2 > IDIC3 > IDIC6 > IDIC1 > IDIC5 > IDICR > IDIC4. The calculated  $\lambda_e$  value for IDICR is 0.00047988 eV and those for IDIC1–IDIC6 are 0.00022499, -0.00253835, -0.00200788, 0.00052472, 0.00056658, and -0.00330809 eV, respectively. The decreasing order of  $\lambda_e$  for title compounds is IDIC5 > IDIC4 > IDICR > IDIC1 > IDIC3 > IDIC2 > IDIC6. Overall, the study reveals that the  $\lambda_e$  values of all title molecules are smaller than  $\lambda_h$  values, except for the reference and IDIC5 and IDIC4, which stipulates that all titled chromophores are captivating candidates for transfer of electrons.

**Open Circuit Voltage ( $V_{\text{oc}}$ ) Investigation.** The performance of OSCs is highlighted using open circuit tension ( $V_{\text{oc}}$ ).<sup>44</sup> In fact, it explains the greatest quantity of current from any optical material.<sup>45</sup> The influence of  $V_{\text{oc}}$  can be determined by different parameters: recombination of charge carriers, external fluorescence, light source, OSC temperature, electrode function, light intensity, and numerous environmental factors. The open circuit voltage is directly associated with the energy difference of HOMO and LUMO of A and D molecules, i.e.,  $\text{HOMO}_{\text{donor}} - \text{LUMO}_{\text{acceptor}}$ . In the current investigation, a renowned donor polymer PBDB-T<sup>46</sup> is utilized for calculating

the open circuit values and -4.936 eV is the simulated  $E_{\text{HOMO}}$  value for the donor polymer. Theoretically, the examined outcomes of  $V_{\text{oc}}$  of the OSCs are determined using eq 3, reported by Scharber and co-workers,<sup>47</sup> and results are exhibited in Table 5.

$$V_{\text{oc}} = (|E_{\text{HOMO}}^{\text{D}}| - |E_{\text{LUMO}}^{\text{A}}|) - 0.3 \quad (3)$$

**Table 5. Energy Driving Force and Open Circuit Voltage of Titled Compounds<sup>a</sup>**

compounds	$\Delta E$ (eV)	$V_{\text{oc}}$ (V)
IDICR	1.233	0.933
IDIC1	1.087	0.787
IDIC2	0.832	0.532
IDIC3	0.782	0.482
IDIC4	1.209	0.909
IDIC5	1.151	0.851
IDIC6	0.378	0.078

<sup>a</sup> $\Delta E = E_{\text{LUMO}}^{\text{A}} - E_{\text{HOMO}}^{\text{D}}$ .

The values of  $V_{\text{oc}}$  for IDICR and IDIC1–IDIC6 regarding the difference in energy of  $\text{HOMO}_{\text{PBDB-T}} - \text{LUMO}_{\text{ACCEPTOR}}$  are noted to be 0.933, 0.787, 0.532, 0.482, 0.909, 0.851, and 0.078 V, respectively. Interestingly, the computed open circuit voltage value of the reference chromophore showed excellent agreement with experimentally determined results (0.97 V).<sup>28</sup> All our derivatives exhibited a comparable value of voltage with that of the parent chromophore. Among the designed compounds, IDIC4 with reference to the energy difference of  $\text{HOMO}_{\text{donor}}$  exhibited a greater  $V_{\text{oc}}$  value of 0.909 V. The  $V_{\text{oc}}$  results of title compounds are found to be in the decreasing order of IDICR > IDIC4 > IDIC5 > IDIC1 > IDIC2 > IDIC3 > IDIC6. As previously stated, the  $V_{\text{oc}}$  value mostly depends upon the level of HOMO of D and LUMO of A. Lower acceptor origin LUMO results in a higher  $V_{\text{oc}}$  value and improved optoelectronic parameters. The movement of electrons from HOMO of D molecules is increased by a low-lying LUMO of acceptor, which directly improves the optoelectronic characteristics. Furthermore, the HOMO–LUMO band gap between the acceptor and donor units amplifies PEC values. As a result, Figure 6 depicts the orbital energy diagram of the aforesaid chromophores in relation to PBDB-T. Figure 6 shows that the LUMO level of the donor

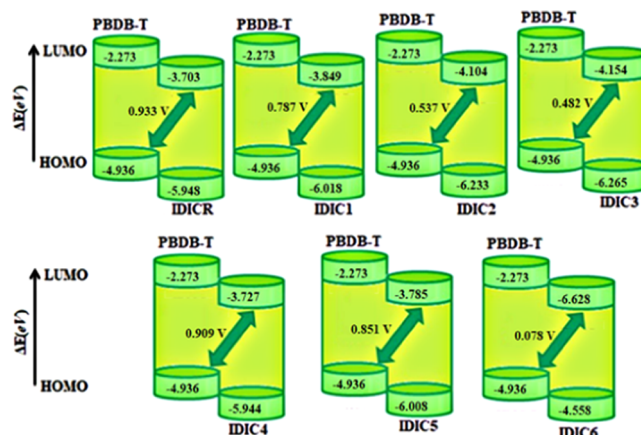


**Figure 6.** Graphical representation of  $V_{\text{oc}}$  for IDICR and IDIC1–IDIC6 with PBDB-T.

polymer PBDB-T lies higher than the LUMO level of the acceptor chromophores. This makes it easier to transfer electrons from the donor polymer to the acceptor segment, which improves the studied molecular optoelectronic parameters.

**Charge Transfer Analysis.** To explore the potential utilization of titled chromophores in the charge transfer for OSC materials, IDIC5 acceptor molecule was blended with PBDB-T donor polymer, and the complex was optimized at B3LYP functional with the 6-31G(d,p) basis set. PBDB-T is a well-known polymeric-natured chromophore that is often employed in CT analysis.<sup>46</sup> The optimized structure of the PBDB-T: IDIC5 complex is presented in Figure 7a. To

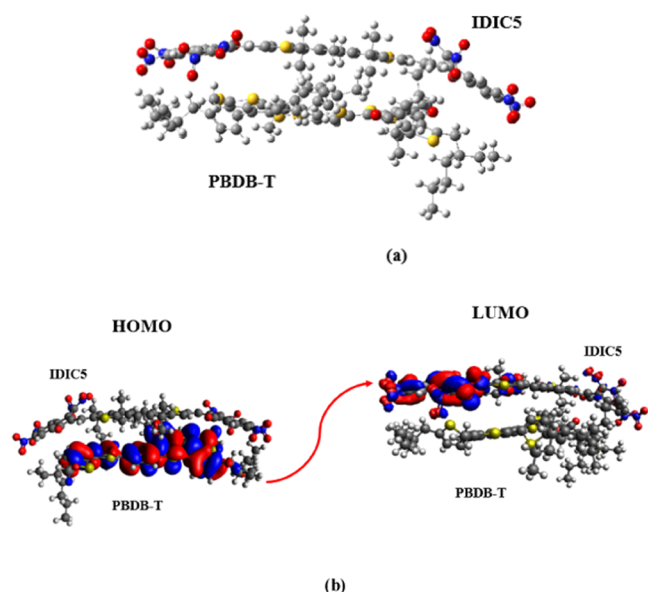


**Figure 7.** Optimized geometry of PBDB-T:IDIC5 complex (a) and charge transfer phenomenon between PBDB-T donor polymer and IDIC5 chromophore (b).

observe the effective transfer of charge, we placed our designed chromophore parallel to the donor (PBDB-T) polymer. Figure 7b reveals that an efficient electronic cloud is concentrated over PBDB-T for HOMO, while for LUMO, it is located over the end-capped acceptor moieties of IDIC5. An effective transfer of electrons from donor to acceptor indicated that our derivatives are suitable OSCs that can be significantly utilized for optoelectronic devices.

**Transition Density Matrix Investigation.** Transition density matrix (TDM) calculation is employed for the elucidation of transition processes in the abovementioned compounds. The estimation of the behavior of transitions, specifically from the ground state ( $S_0$ ) to an excited state ( $S_1$ ), as well as donor–acceptor unit interaction and electron–hole localization, was performed utilizing B3LYP/6-311G(d,p) functional. The effect of hydrogen atoms is omitted since it has a negligible impact on these transitions. To accomplish TDM analysis, we divided the titled chromophores (IDICR and IDIC1–IDIC6) into two parts: end-capped acceptor (A) and the central donor (D) moiety, which are depicted in Figure 8 in red and green, respectively. In all of the studied chromophores, the TDM heat maps revealed effective diagonal charge transport coherence. Effective coherent transmission of electrons was conducted from D to A, allowing for good

electron density shifting without any trapping. TDM heat maps imply an easier and higher exciton dissociation in the excited state, which is very convenient for solar cell development.

**Exciton Binding Energy ( $E_b$ ) Analysis.** Binding energy is considered a significant aspect for estimation of photovoltaic properties obtained from OSCs, which aids in the explanation of exciton dissociation capacity.<sup>48,49</sup> The binding energy of holes and electrons is a notable metric for explicating the interaction due to Coulombic force. A smaller Coulombic force interplay between holes and electrons with larger exciton dissociation in the excited state  $E_{opt}$  refers to the  $S_0$  to  $S_1$  state energies.<sup>50,51</sup> Using eq 4, the binding energy of titled chromophores is calculated in Table 6.

$$E_b = E_{H-L} - E_{opt} \quad (4)$$

All theoretical molecules showed comparable  $E_b$  with their parent chromophores (IDICR). This reduction in  $E_b$  showed the excited state to possess greater exciton dissociation. The binding energy of the designed molecules is shown in decreasing order as IDIC5 = IDIC4 > IDIC2 = IDIC1 > IDIC3 > IDIC6 > IDICR. Among all title chromophores, IDIC6 exhibited a reduced value of binding energy that described superior optoelectronic properties with the greatest efficiency in exciton dissociation. The chromophore derivatives with 1.9 eV  $E_b$  are observed to be the perfect OSC structures with efficient  $V_{oc}$ . Interestingly, all of our studied chromophores have binding energy lower than 1.9 eV, illustrating them as perfect NF-OSCs.

## CONCLUSIONS

In the present study, a donor indacenodithiophene (IDT)-based core with A–D–A architecture non-fullerene IDICR chromophore has been quantum chemically designed by end-capped modifications to make efficient photovoltaic material. Various kinds of strong electron-withdrawing groups have been introduced by the structural tailoring of “A” moieties to obtain larger bathochromic shifts with a narrow energy gap. Frontier molecular orbital (FMO), density of state (DOS), and transition density matrix (TDM) investigations are explored, and as a result, the IDT core is found to play a critical role in the transfer of charge from HOMO to LUMO. Further,  $V_{oc}$  has also been estimated with regard to  $HOMO_{PBDB-T} - LUMO_{Acceptor}$  and their data is found to be in the order IDICR (0.933 V) > IDIC4 (0.909 V) > IDIC5 (0.851 V) > IDIC1 (0.787 V) > IDIC2 (0.532 V) > IDIC3 (0.482 V) > IDIC6 (0.078 V). Interestingly, smaller binding energy ( $E_b$ ) (0.309–0.224 eV) of the abovementioned chromophores was determined, which resulted in greater excitation dissociation. Subsequently, greater excitation dissociation predicted the larger power conversion efficiency of chromophores. It has been concluded that all of the aforementioned chromophores obtained by structural modification could be alluring as effective, economically viable OSC materials with multiple features and are also interesting for synthetic researchers.

## METHODS

All of the computations were executed using Gaussian version 09 software.<sup>52</sup> For obtaining the optimized geometrical structures of IDICR, density functional theory (DFT) investigations were executed at different functionals, B3LYP,<sup>53</sup> CAM-B3LYP,<sup>54</sup> M06-2X,<sup>55</sup> and  $\omega$ B97XD,<sup>56</sup> with the 6-311G(d,p) basis set. Further, UV–visible examinations

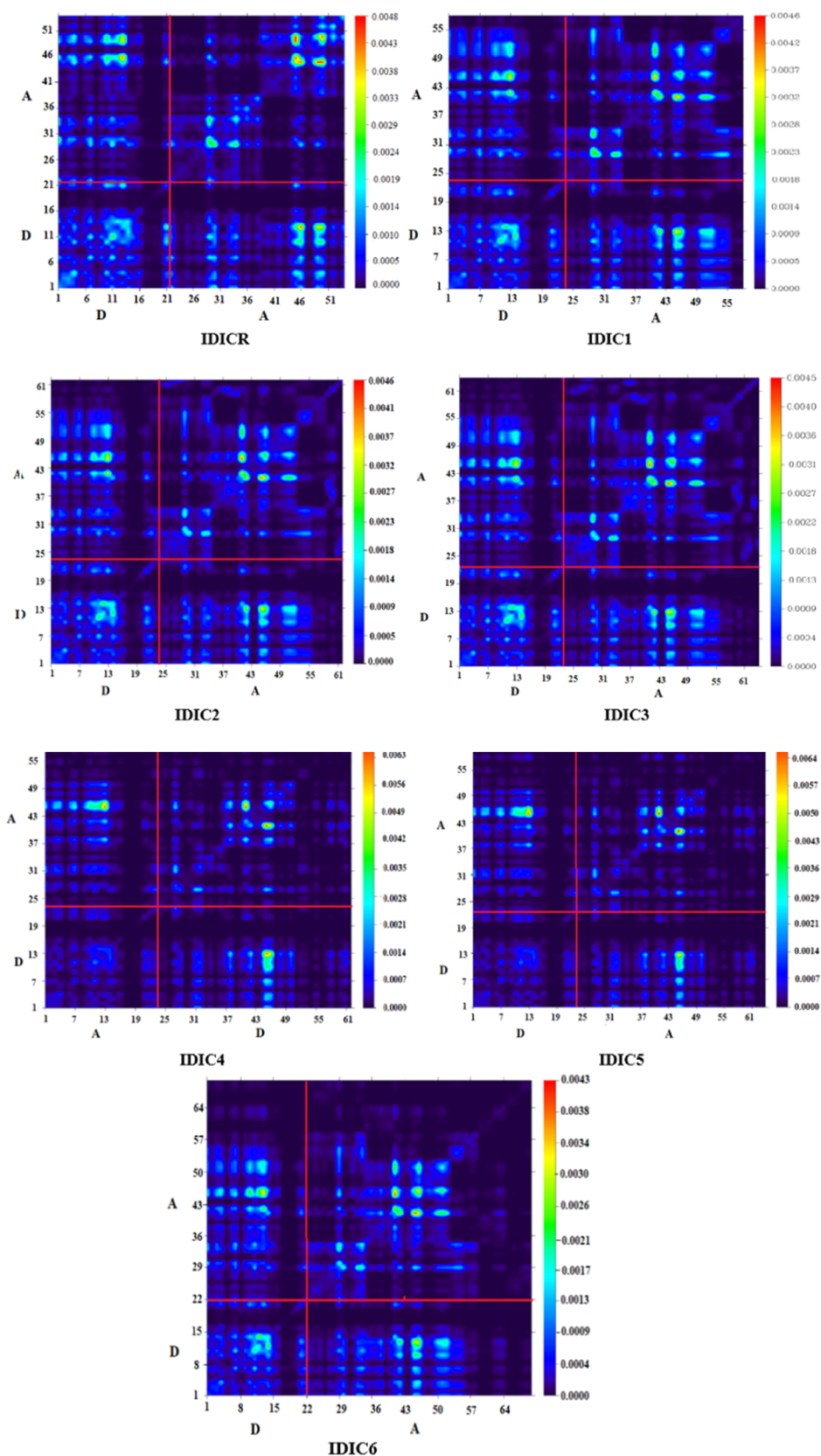


Figure 8. TDM of studied compounds at the S1 state.

in chloroform for IDICR were carried out at the above-mentioned functionals and basis set (Figure 9). At the B3LYP level, absorption spectra of DFT-based results were noted to be in agreement with the experimental values<sup>28</sup> (Figure 9). To

investigate the configuration and optoelectronic properties of OSCs, IDIC1–IDIC6 were optimized at the B3LYP level of theory. Further, their density of states (DOS), absorption spectra, open circuit voltage ( $V_{oc}$ ), reorganization energy (RE),

Table 6. Calculated  $E_{H-L}$ ,  $E_{opt}$ , and  $E_b$  of Titled Chromophores

compounds	$E_{H-L}$ (eV)	$E_{opt}$ (eV)	$E_b$ (eV)
IDICR	2.245	2.021	0.224
IDIC1	2.169	1.929	0.24
IDIC2	2.129	1.888	0.241
IDIC3	2.111	1.874	0.237
IDIC4	2.217	1.913	0.304
IDIC5	2.223	1.914	0.309
IDIC6	2.070	1.838	0.232

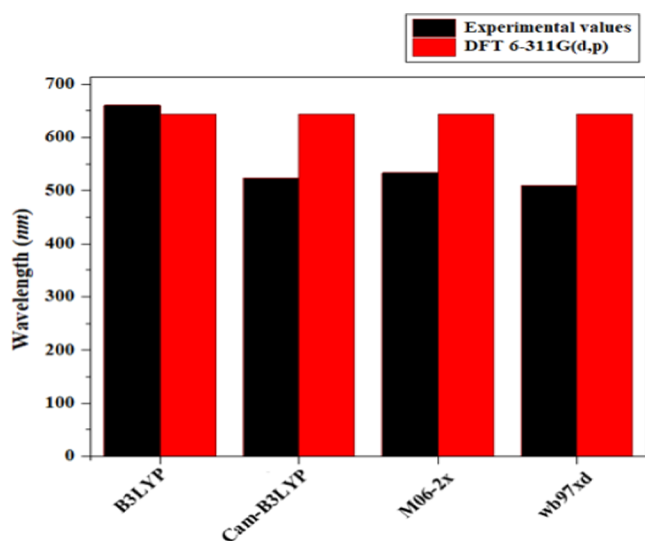


Figure 9. Simulated UV-vis results of IDICR at various levels in chloroform solvent.

frontier molecular orbital (FMO) analysis, binding energy ( $E_b$ ), and transition density matrix (TDM) were studied at the aforesaid functional. Many kinds of software such as Multiwfn version 3.8,<sup>57</sup> PyMolyze version 2.0,<sup>58</sup> Avogadro version 1.2.0n,<sup>59</sup> Gaussview version 5.0,<sup>60</sup> and Chemcraft<sup>61</sup> were utilized for interpretation of data. We are thankful to Prof. A.A.C.B from IQ-USP, Brazil, for the cooperation and collaboration, especially for his continuous support and providing computational laboratory facilities.

## ■ ASSOCIATED CONTENT

### SI Supporting Information

The Supporting Information is available free of charge at <https://pubs.acs.org/doi/10.1021/acsomega.1c06219>.

Cartesian coordinates; UV-vis data (wavelengths, excitation energies, and oscillator strengths); synthesis pathway of IDICR chromophore; and Gibbs free energy of reported chromophores calculated using B3LYP/6-311G (d,p) (PDF)

## ■ AUTHOR INFORMATION

### Corresponding Author

Muhammad Khalid – Department of Chemistry, Khwaja Fareed University of Engineering & Information Technology, Rahim Yar Khan 64200, Pakistan; [orcid.org/0000-0002-1899-5689](https://orcid.org/0000-0002-1899-5689); Email: [khalid@iq.usp.br](mailto:khalid@iq.usp.br), [muhammad.khalid@kfueit.edu.pk](mailto:muhammad.khalid@kfueit.edu.pk), [khalidhej@hotmail.com](mailto:khalidhej@hotmail.com)

## Authors

Muhammad Nadeem Arshad – Chemistry Department, Faculty of Science, King Abdulaziz University, Jeddah 21589, Saudi Arabia; Center of Excellence for Advanced Material Research (CEAMR), King Abdulaziz University, Jeddah 21589, Saudi Arabia

Iqra Shafiq – Department of Chemistry, Khwaja Fareed University of Engineering & Information Technology, Rahim Yar Khan 64200, Pakistan

Abdullah M. Asiri – Chemistry Department, Faculty of Science, King Abdulaziz University, Jeddah 21589, Saudi Arabia; Center of Excellence for Advanced Material Research (CEAMR), King Abdulaziz University, Jeddah 21589, Saudi Arabia; [orcid.org/0000-0001-7905-3209](https://orcid.org/0000-0001-7905-3209)

Complete contact information is available at:

<https://pubs.acs.org/doi/10.1021/acsomega.1c06219>

## Notes

The authors declare no competing financial interest.

## ■ ACKNOWLEDGMENTS

This project was funded by the Deanship of Scientific Research (DSR) at King Abdulaziz University, Jeddah, under grant no. (G:309-130-1442). The authors, therefore, acknowledge with thanks DSR for technical and financial support.

## ■ REFERENCES

- (1) Li, G.; Zhu, R.; Yang, Y. Polymer Solar Cells. *Nat. Photonics* **2012**, *6*, 153–161.
- (2) Yan, C.; Barlow, S.; Wang, Z.; Yan, H.; Jen, A. K.-Y.; Marder, S. R.; Zhan, X. Non-Fullerene Acceptors for Organic Solar Cells. *Nat. Rev. Mater.* **2018**, *3*, No. 18003.
- (3) Cheng, P.; Li, G.; Zhan, X.; Yang, Y. Next-Generation Organic Photovoltaics Based on Non-Fullerene Acceptors. *Nat. Photonics* **2018**, *12*, 131–142.
- (4) Lu, L.; Zheng, T.; Wu, Q.; Schneider, A. M.; Zhao, D.; Yu, L. Recent Advances in Bulk Heterojunction Polymer Solar Cells. *Chem. Rev.* **2015**, *115*, 12666–12731.
- (5) Yu, G.; Gao, J.; Hummelen, J. C.; Wudl, F.; Heeger, A. J. Polymer Photovoltaic Cells: Enhanced Efficiencies via a Network of Internal Donor-Acceptor Heterojunctions. *Science* **1995**, *270*, 1789–1791.
- (6) Chiang, C.-H.; Wu, C.-G. Bulk Heterojunction Perovskite-PCBM Solar Cells with High Fill Factor. *Nat. Photonics* **2016**, *10*, 196–200.
- (7) Xu, X.; Yu, T.; Bi, Z.; Ma, W.; Li, Y.; Peng, Q. Realizing over 13% Efficiency in Green-Solvent-Processed Nonfullerene Organic Solar Cells Enabled by 1, 3, 4-Thiadiazole-Based Wide-Bandgap Copolymers. *Adv. Mater.* **2018**, *30*, No. 1703973.
- (8) Deng, D.; Zhang, Y.; Zhang, J.; Wang, Z.; Zhu, L.; Fang, J.; Xia, B.; Wang, Z.; Lu, K.; Ma, W.; Wei, Z. Fluorination-Enabled Optimal Morphology Leads to over 11% Efficiency for Inverted Small-Molecule Organic Solar Cells. *Nat. Commun.* **2016**, *7*, No. 13740.
- (9) Liu, T.; Troisi, A. What Makes Fullerene Acceptors Special as Electron Acceptors in Organic Solar Cells and How to Replace Them. *Adv. Mater.* **2013**, *25*, 1038–1041.
- (10) Anctil, A.; Babbitt, C. W.; Raffaele, R. P.; Landi, B. J. Material and energy intensity of fullerene production. *Environ. Sci. Technol.* **2011**, *45*, 2353–2359.
- (11) He, Y.; Li, Y. Fullerene derivative acceptors for high performance polymer solar cells. *Phys. Chem. Chem. Phys.* **2011**, *13*, 1970–1983.
- (12) Lin, Y.; Wang, J.; Zhang, Z.-G.; Bai, H.; Li, Y.; Zhu, D.; Zhan, X. An Electron Acceptor Challenging Fullerenes for Efficient Polymer Solar Cells. *Adv. Mater.* **2015**, *27*, 1170–1174.

- (13) Lin, Y.; Zhan, X. Oligomer Molecules for Efficient Organic Photovoltaics. *Acc. Chem. Res.* **2016**, *49*, 175–183.
- (14) Etxebarria, I.; Ajuria, J.; Pacios, R. Solution-Processable Polymer Solar Cells: A Review on Materials, Strategies and Cell Architectures to Overcome 10%. *Org. Electron.* **2015**, *19*, 34–60.
- (15) Qi, Q.; Guo, X.; Zhu, B.; Deng, P.; Zhan, H.; Yang, J. Side-Chain Optimization of Perylene Diimide-Thiophene Random Terpolymer Acceptors for Enhancing the Photovoltaic Efficiency of All-Polymer Solar Cells. *Org. Electron.* **2020**, *78*, No. 105616.
- (16) Wang, H.; Li, M.; Liu, Y.; Song, J.; Li, C.; Bo, Z. Perylene Diimide Based Star-Shaped Small Molecular Acceptors for High Efficiency Organic Solar Cells. *J. Mater. Chem. C* **2019**, *7*, 819–825.
- (17) Liu, Z.; Zeng, D.; Gao, X.; Li, P.; Zhang, Q.; Peng, X. Non-Fullerene Polymer Acceptors Based on Perylene Diimides in All-Polymer Solar Cells. *Sol. Energy Mater. Sol. Cells* **2019**, *189*, 103–117.
- (18) Liu, X.; Kong, F.; Guo, F.; Cheng, T.; Chen, W.; Yu, T.; Chen, J.; Tan, Z.; Dai, S. Influence of  $\pi$ -Linker on Triphenylamine-Based Hole Transporting Materials in Perovskite Solar Cells. *Dyes Pigm.* **2017**, *139*, 129–135.
- (19) Feng, H.; Qiu, N.; Wang, X.; Wang, Y.; Kan, B.; Wan, X.; Zhang, M.; Xia, A.; Li, C.; Liu, F.; Zhang, H.; Chen, Y. An ADA Type Small-Molecule Electron Acceptor with End-Extended Conjugation for High Performance Organic Solar Cells. *Chem. Mater.* **2017**, *29*, 7908–7917.
- (20) Li, Y.; Lin, J.-D.; Che, X.; Qu, Y.; Liu, F.; Liao, L.-S.; Forrest, S. R. High Efficiency Near-Infrared and Semitransparent Non-Fullerene Acceptor Organic Photovoltaic Cells. *J. Am. Chem. Soc.* **2017**, *139*, 17114–17119.
- (21) Lin, Y.; Zhao, F.; He, Q.; Huo, L.; Wu, Y.; Parker, T. C.; Ma, W.; Sun, Y.; Wang, C.; Zhu, D.; et al. High-Performance Electron Acceptor with Thieryl Side Chains for Organic Photovoltaics. *J. Am. Chem. Soc.* **2016**, *138*, 4955–4961.
- (22) Meng, L.; Zhang, Y.; Wan, X.; Li, C.; Zhang, X.; Wang, Y.; Ke, X.; Xiao, Z.; Ding, L.; Xia, R.; et al. Organic and Solution-Processed Tandem Solar Cells with 17.3% Efficiency. *Science* **2018**, *361*, 1094–1098.
- (23) Bibi, S.; Li, P.; Zhang, J. X-Shaped Donor Molecules Based on Benzo [2, 1-b: 3, 4-B'] Dithiophene as Organic Solar Cell Materials with PDIs as Acceptors. *J. Mater. Chem. A* **2013**, *1*, 13828–13841.
- (24) Zhang, J.; Li, G.; Kang, C.; Lu, H.; Zhao, X.; Li, C.; Li, W.; Bo, Z. Synthesis of Star-Shaped Small Molecules Carrying Peripheral 1, 8-Naphthalimide Functional Groups and Their Applications in Organic Solar Cells. *Dyes Pigm.* **2015**, *115*, 181–189.
- (25) Sun, Y.; Welch, G. C.; Leong, W. L.; Takacs, C. J.; Bazan, G. C.; Heeger, A. J. Solution-Processed Small-Molecule Solar Cells with 6.7% Efficiency. *Nat. Mater.* **2012**, *11*, 44–48.
- (26) Suman, S.; Singh, S. P. Impact of End Groups on the Performance of Non-Fullerene Acceptors for Organic Solar Cell Applications. *J. Mater. Chem. A* **2019**, *7*, 22701–22729.
- (27) Khalid, M.; Khan, M. U.; Razia, E.; Shafiq, Z.; Alam, M. M.; Imran, M.; Akram, M. S. Exploration of Efficient Electron Acceptors for Organic Solar Cells: Rational Design of Indacenodithiophene Based Non-Fullerene Compounds. *Sci. Rep.* **2021**, *11*, No. 19931.
- (28) Zhang, Y.; et al. Tuning the molecular geometry and packing mode of non-fullerene acceptors by altering the bridge atoms towards efficient organic solar cells. *Mater. Chem. Front.* **2020**, *4*, 2462–2471.
- (29) Zhang, Y.; Liu, Z.; Shan, T.; Wang, Y.; Zhu, L.; Li, T.; Liu, F.; Zhong, H. Tuning the Molecular Geometry and Packing Mode of Non-Fullerene Acceptors by Altering the Bridge Atoms towards Efficient Organic Solar Cells. *Mater. Chem. Front.* **2020**, *4*, 2462–2471.
- (30) Srncic, M.; Solomon, E. I. Frontier Molecular Orbital Contributions to Chlorination versus Hydroxylation Selectivity in the Non-Heme Iron Halogenase SyrB2. *J. Am. Chem. Soc.* **2017**, *139*, 2396–2407.
- (31) Gunasekaran, S.; Balaji, R. A.; Kumeresan, S.; Anand, G.; Srinivasan, S. Experimental and Theoretical Investigations of Spectroscopic Properties of N-Acetyl-5-Methoxytryptamine. *Can. J. Anal. Sci. Spectrosc.* **2008**, *53*, 149–162.
- (32) Soleimani Amiri, S.; Makarem, S.; Ahmar, H.; Ashenagar, S. Theoretical Studies and Spectroscopic Characterization of Novel 4-Methyl-5-((5-Phenyl-1, 3, 4-Oxadiazol-2-Yl) Thio) Benzene-1, 2-Diol. *J. Mol. Struct.* **2016**, *1119*, 18–24.
- (33) Khan, M. U.; Khalid, M.; Ibrahim, M.; Braga, A. A. C.; Safdar, M.; Al-Saadi, A. A.; Janjua, M. R. S. A First Theoretical Framework of Triphenylamine–Dicyanovinylene-Based Nonlinear Optical Dyes: Structural Modification of  $\pi$ -Linkers. *J. Phys. Chem. C* **2018**, *122*, 4009–4018.
- (34) Khan, M. U.; Ibrahim, M.; Khalid, M.; Qureshi, M. S.; Gulzar, T.; Zia, K. M.; Al-Saadi, A. A.; Janjua, M. R. S. A First Theoretical Probe for Efficient Enhancement of Nonlinear Optical Properties of Quinacridone Based Compounds through Various Modifications. *Chem. Phys. Lett.* **2019**, *715*, 222–230.
- (35) Khan, M. U.; et al. Prediction of second-order nonlinear optical properties of D- $\pi$ -A compounds containing novel fluorene derivatives: a promising route to giant hyperpolarizabilities. *J. Cluster Sci.* **2019**, *30*, 415–430.
- (36) Khan, M. U.; Ibrahim, M.; Khalid, M.; Jamil, S.; Al-Saadi, A. A.; Janjua, M. R. S. A Quantum Chemical Designing of Indolo [3, 2, 1-Jk] Carbazole-Based Dyes for Highly Efficient Nonlinear Optical Properties. *Chem. Phys. Lett.* **2019**, *719*, 59–66.
- (37) Afzal, Z.; Hussain, R.; Khan, M. U.; Khalid, M.; Iqbal, J.; Alvi, M. U.; Adnan, M.; Ahmed, M.; Mehboob, M. Y.; Hussain, M.; Tariq, C. J. Designing Indenothiophene-Based Acceptor Materials with Efficient Photovoltaic Parameters for Fullerene-Free Organic Solar Cells. *J. Mol. Model.* **2020**, *26*, 1–17.
- (38) Hussain, R.; Khan, M. U.; Mehboob, M. Y.; Khalid, M.; Iqbal, J.; Ayub, K.; Adnan, M.; Ahmed, M.; Atiq, K.; Mahmood, K. Enhancement in Photovoltaic Properties of N, N-Diethylaniline Based Donor Materials by Bridging Core Modifications for Efficient Solar Cells. *ChemistrySelect* **2020**, *5*, 5022–5034.
- (39) Yao, C.; Yang, Y.; Li, L.; Bo, M.; Zhang, J.; Peng, C.; Huang, Z.; Wang, J. Elucidating the Key Role of the Cyano (-C $\equiv$ N) Group to Construct Environmentally Friendly Fused-Ring Electron Acceptors. *J. Phys. Chem. C* **2020**, *124*, 23059–23068.
- (40) Hussain, S.; Hussain, R.; Mehboob, M. Y.; Chatha, S. A. S.; Hussain, A. I.; Umar, A.; Khan, M. U.; Ahmed, M.; Adnan, M.; Ayub, K. Adsorption of Phosgene Gas on Pristine and Copper-Decorated B12N12 Nanocages: A Comparative DFT Study. *ACS Omega* **2020**, *5*, 7641–7650.
- (41) Hussain, S.; Chatha, S. A. S.; Hussain, A. I.; Hussain, R.; Mehboob, M. Y.; Muhammad, S.; Ahmad, Z.; Ayub, K. Zinc-Doped Boron Phosphide Nanocluster as Efficient Sensor for SO<sub>2</sub>. *J. Chem.* **2020**, *2020*, No. 2629596.
- (42) Khan, M. U.; Khalid, M.; Hussain, R.; Umar, A.; Mehboob, M. Y.; Shafiq, Z.; Imran, M.; Irfan, A. Novel W-shaped oxygen heterocycle-fused fluorene-based non-fullerene acceptors: first theoretical framework for designing environment-friendly organic solar cells. *Energy Fuels* **2021**, *35*, 12436–12450.
- (43) Ans, M.; Iqbal, J.; Ayub, K.; Ali, E.; Eliasson, B. Spirobifluorene Based Small Molecules as an Alternative to Traditional Fullerene Acceptors for Organic Solar Cells. *Mater. Sci. Semicond. Process.* **2019**, *94*, 97–106.
- (44) Irfan, M.; Iqbal, J.; Sadaf, S.; Eliasson, B.; Rana, U. A.; Ud-din Khan, S.; Ayub, K. Design of Donor–Acceptor–Donor (D–A–D) Type Small Molecule Donor Materials with Efficient Photovoltaic Parameters. *J. Quantum Chem.* **2017**, *117*, No. e25363.
- (45) Tang, S.; Zhang, J. Design of Donors with Broad Absorption Regions and Suitable Frontier Molecular Orbitals to Match Typical Acceptors via Substitution on Oligo (Thienylenevinylene) toward Solar Cells. *J. Comput. Chem.* **2012**, *33*, 1353–1363.
- (46) Zheng, Z.; Yao, H.; Ye, L.; Xu, Y.; Zhang, S.; Hou, J. PBDB-T and Its Derivatives: A Family of Polymer Donors Enables over 17% Efficiency in Organic Photovoltaics. *Mater. Today* **2020**, *35*, 115–130.
- (47) Scharber, M. C.; Mühlbacher, D.; Koppe, M.; Denk, P.; Waldauf, C.; Heeger, A. J.; Brabec, C. J. Design Rules for Donors in Bulk-Heterojunction Solar Cells—Towards 10% Energy-Conversion Efficiency. *Adv. Mater.* **2006**, *18*, 789–794.

- (48) Kraner, S.; Prampolini, G.; Cuniberti, G. Exciton Binding Energy in Molecular Triads. *J. Chem. Phys. C* **2017**, *121*, 17088–17095.
- (49) Kraner, S.; Scholz, R.; Plasser, F.; Koerner, C.; Leo, K. Exciton Size and Binding Energy Limitations in One-Dimensional Organic Materials. *J. Phys. Chem. A* **2015**, *143*, No. 244905.
- (50) Dkhissi, A. Excitons in Organic Semiconductors. *Synth. Met.* **2011**, *161*, 1441–1443.
- (51) Köse, M. E. Evaluation of Acceptor Strength in Thiophene Coupled Donor–Acceptor Chromophores for Optimal Design of Organic Photovoltaic Materials. *J. Phys. Chem. A* **2012**, *116*, 12503–12509.
- (52) Frisch, M. J.; Trucks, G. W.; Schlegel, H. B.; Scuseria, G. E.; Robb, M. A.; Cheeseman, J. R.; Scalmani, G.; Barone, V.; Mennucci, B.; Petersson, G. A. *Gaussian 09*, revision ABCD. 0123; Gaussian, Inc.: Wallingford CT, 2013.
- (53) Civaleri, B.; Zicovich-Wilson, C. M.; Valenzano, L.; Ugliengo, P. B3LYP Augmented with an Empirical Dispersion Term (B3LYP-D\*) as Applied to Molecular Crystals. *CrystEngComm* **2008**, *10*, 405–410.
- (54) Yanai, T.; Tew, D. P.; Handy, N. C. A New Hybrid Exchange–Correlation Functional Using the Coulomb-Attenuating Method (CAM-B3LYP). *Chem. Phys. Lett.* **2004**, *393*, 51–57.
- (55) Walker, M.; Harvey, A. J.; Sen, A.; Dessent, C. E. Performance of M06, M06-2X, and M06-HF Density Functionals for Conformationally Flexible Anionic Clusters: M06 Functionals Perform Better than B3LYP for a Model System with Dispersion and Ionic Hydrogen-Bonding Interactions. *J. Phys. Chem. A* **2013**, *117*, 12590–12600.
- (56) Altalhi, T. A.; Ibrahim, M. M.; Gobouri, A. A.; El-Sheshtawy, H. S. Exploring Non-Covalent Interactions for Metformin-Thyroid Hormones Stabilization: Structure, Hirshfeld Atomic Charges and Solvent Effect. *J. Mol. Liq.* **2020**, *313*, No. 113590.
- (57) Lu, T.; Chen, F. Multiwfn: a multifunctional wavefunction analyzer. *J. Comput. Chem.* **2012**, *33*, 580–592.
- (58) O'boyle, N. M.; Tenderholt, A. L.; Langner, K. M. Cclib: A Library for Package-Independent Computational Chemistry Algorithms. *J. Comput. Chem.* **2008**, *29*, 839–845.
- (59) Hanwell, M. D.; Curtis, D. E.; Lonie, D. C.; Vandermeersch, T.; Zurek, E.; Hutchison, G. R. Avogadro: An Advanced Semantic Chemical Editor, Visualization, and Analysis Platform. *J. Cheminformatics* **2012**, *4*, No. 17.
- (60) Dennington, R. D.; Keith, T. A.; Millam, J. M. GaussView 5.0. Gaussian, Inc.: Wallingford 2008.
- (61) Zhurko, G. A.; Zhurko, D. A. ChemCraft, version 1.6. URL: <http://www.chemcraftprog.com> 2009.